Korean Journal of Oral and Maxillofacial Pathology 2020;44(4):103-112
ISSN:1225-1577(Print); 2384-0900(Online)
Available online at http://journal.kaomp.org
https://doi.org/10.17779/KAOMP.2020.44.4.001

SAMP1/Klotho-결핍 마우스의 하악골에서 골형성이상

육종인[1], Nguyen Khanh Toan[2], 서요섭[3], 유상준[4], 안상건[2]*

연세대학교 치과대학 구강병리학교실[1]
조선대학교 치과대학 구강병리학교실[2]
조선대학교 치과대학 구강악안면방사선학교실[3]
조선대학교 치과대학 치주과학교실[4]

〈Abstract〉

Dysosteogenesis in the Mandibular Bone of SAMP1/Klotho-Deficient Mice

*Jong-In Yook[1], Nguyen Khanh Toan[2], Yo-Seob Seo[3], Sang-Joun Yu[4] and Sang-Gun Ahn[2]**

[1]Department of Oral Pathology, College of Dentistry, Yonsei University, Seoul 03722
[2]Department of Oral Pathology, School of Dentistry, Chosun University, Gwangju 61452
[3]Department of Oral and Maxillofacial Radiology, School of Dentistry, Chosun University
[4]Department of Periodontology, School of Dentistry, Chosun University, Gwangju 61452, Republic of Korea

Aging is a physiological change that leads to a decline in biological functions from metabolic stress. To investigate the effect of aging on mandibular bone formation, we created SAMP1/Klotho-deficient mice and performed micro-computed tomography (micro-CT) and histology analyses in 4-or 8 week-old SAMP1/kl -/- mice. SAMP1/kl -/- mice exhibited extensive inflammation, tissue calcification, and abnormal mandibular bone development. Using micro-CT analysis, SAMP1/kl -/- mice displayed a loss of incisor roots and irregular dentinal tubule formation, as well as calcification within the pulp root canal. Furthermore, the mandibular ramus showed extensive ground glass appearance in SAMP1/kl -/- mice. In histological analysis, we found calcified skeletal structures and dysplastic bone formation in SAMP1/kl -/- mice. These results provide an understanding of the pathologic alterations of aging-related mandibular bone. SAMP1/kl -/- mice may serve as a novel model for dysosteogenesis in mandibular bone development.

Key words: SAMP1/ Klotho, Aging, Dysosteogenesis, Mandibular bone, Bone development

Ⅰ. INTRODUCTION

Aging is characterized by a progressive decline in the physiological function/homeostasis eventually leading to morbidity and mortality[1]. During the aging process, age-related bone loss in terms of composition, skeletal structure and function predispose to osteoporosis[2]. The deterioration in bone mass is a major phenotype of accelerated aging and induces bone dysfunction together with vulnerability to additional diseases. Because of the close relationship between the aging process and pathogenesis in bone, basic and clinical research of age-related bone loss has increased significantly in recent years[3-5].

Klotho is a transmembrane protein that functions as an aging suppressor or anti-senescence-related protein and plays

* Correspondence: Sang-Gun Ahn, Department of Pathology, School of Dentistry, Chosun University, #309 Pilmun-Daero, Dong-gu, Gwangju, Republic of Korea, 61452
Tel: +82-62-230-6898, Fax: +82-62-223-3205
E-mail: ahnsg@chosun.ac.kr
ORCID: 0000-0002-5837-7527
Received: Jun. 26. 2020; Revised: Jul. 3. 2020; Accepted: Aug. 7. 2020

a crucial role in phosphate, calcium, and vitamin D metabolism[6,7]. Klotho-deficient mice have identical aging phenotypes such as a short life-span, ectopic calcification, osteoporosis, arteriosclerosis, muscle atrophy, and skin atrophy[5,8]. In the kidney, Klotho deficiency induces severe hyperphosphatemia and hypervitaminosis D through impaired FGF23 signaling[6,9]. Furthermore, Klotho can also activate the calcium channels transient receptor potential vanilloid receptor (TRPV) 5/6 and conserve serum calcium and reduce calciuria[7]. Klotho is involved in the IGF-1/IGFR, Wnt and transforming growth factor-β (TGF-β) signaling pathways[10,11]. Recent studies observed direct effects of Klotho on bone formation and remodeling[12,13]. Klotho -/- mice show low bone mineral formation and bone resorption activities, and bone metabolism, which result in osteodysplasia and/or osteoporosis that are characterized by low-bone volume and low-bone turnover[5,13-15]. However, the other studies reported increased trabecular bone volume and thickness or increased bone volume and low-bone turnover in klotho knockout mice[15-17]. Although controversy exists as to the changes in bone formation or bone development, klotho -/- mice exhibited abnormal bone development. However, these findings did not address whether the bone phenotype of klotho -/- mice results from a functional defect of the Klotho gene/proteins or systemic disturbances in bone metabolism associated with aging.

Recently, we created the SAMP1/kl-deficient (SAMP1/kl-/-) mice to more comprehensively explore the complexities of aging[18]. The senescence-accelerated mouse prone 1 (SAMP1) was developed as a mouse model for studying age-related diseases, such as senile amyloidosis, contracted kidneys, an impaired immune response, expansion of the lungs, hearing impairment, and hypertensive vascular disease[19]. We demonstrated that SAMP1/kl-/- mice display atrophy of tissues, growth retardation, and multiple features resembling those associated with premature aging. One of the major features observed in the SAMP1/kl-/- mice was a large amount of ectopic calcification and inflammation in several tissues including the kidney[18].

In this study, micro-CT analysis showed that the mandibular and cortical bones were clearly hypomineralized in SAMP1/kl-/- compared with the age-matched SAMP1/kl+/+. Although the mandibular and cortical bones share morphological features such as mineralization processes, little information is available on how accelerating aging influences tooth and mandibular formation. SAMP1/kl -/- mice displayed a loss of incisor roots and irregular dentinal tubule formation, as well as calcification within the pulp root canal. Defective femur and tibia and abnormal vertebral curvature were also observed at 2 months in SAMP1/kl-/- mice. SAMP1/kl -/- mice may serve as a novel model for dysosteogenesis in mandibular bone development.

Ⅱ. MATERIALS AND METHODS

1. Generation of SAMP1/kl Deficient Mice

Senescence-accelerated mice (SAMP1, 7 weeks old) were purchased from Japan SLC, Inc. (Hamamatsu, Japan). SAM is a group of inbred mouse strains (AKR/J mice) that are used as models to study human aging and age-related diseases[19]. Heterozygous klotho mice (kl+/-) were generously provided by Dr. Kuro-O (University of Texas Southwestern, Dallas, TX, USA). To generate a line of SAMP1/Klotho-deficient mice (SAMP1/kl-/-), we crossed SAMP1 and Klotho heterozygous mice (kl+/-). SAMP1/kl+/+ and SAMP1/kl-/- mice were then derived from SAMP1/kl+/- heterozygous breeding pairs. Tail biopsies were performed for genotyping. DNA was extracted and tested for the presence of wild type and mutant alleles. All animal procedures were performed in accordance with a protocol approved by the Chosun University Institutional Animal Care and Use Committee.

2. Micro-computed tomography imaging

The heads of five male SAMP1/kl-/-mutant mice and of five corresponding age/sex-matched wild-type (WT) littermates were examined at 1 or 2 months of age. All samples were scanned using the Quantum GX micro-CT preclinical in vivo X-ray imaging system (PerkinElmer, Waltham, MA, USA), which operates at an energy of 90 kV and current intensity of 88 μA. Micro-CT data acquisitions (with resolutions at 90, 50, 25, and 25 μm pixel sizes for skulls, mandibles, incisors, and molars, respectively) were reconstructed using advanced microCT analysis software (PerkinElmer, Waltham, MA, USA). Then, according to the region of interest (ROI) selected in the femurs, the characteristics of the trabecular and cortical bone were analyzed by the advanced bone analysis software plug software (PerkinElmer, micro-CT), and a 3D model of the ROI region was constructed by the 3D Optical Imaging software (PerkinElmer, micro-CT).

3. Histology

Samples (heads of 1 or 2-month-old WT and SAMP1/kl-/- mice) were fixed in 10% formalin for 30 days and then transferred into 70% ethanol, washed in water, and demineralized in 10% ethylenediaminetetraacetic acid (EDTA) at 37°C for 10 days (the demineralizing solution was changed every day for the first 3 d and then every other day). After thoroughly washing in water, the heads were dehydrated in graded ethanol, cleared in Histo-Clear (National Diagnostics, Atlanta, GA, USA), and embedded in paraffin at 60°C. Ten-micrometer-thick transverse sections were collected, deparaffinized, and stained with hematoxylin and eosin (H&E).

4. Bone volume analysis

Using the same 3D analysis software, the slice images obtained by micro-CT were reconstructed, and the volume of the femurs was analyzed.

5. Statistical analysis

Statistical analysis was performed with the data obtained from two or three independent experiments. A student's *t*-test was used to analyze protein expression levels and p values less than 0.05 were considered significant. When comparing differences between experimental groups, data were analyzed using ANOVA. The data are represented as the mean ± standard deviation (S.D).

Ⅲ. RESULTS

1. SAMP1/kl-deficient mice displayed severe tooth defects in the proximal incisor region and altered in the mandibular bone

First, we compared the characteristics of the lower incisors between SAMP1/kl+/+ and SAMP1/kl-deficient mice by adding the volumes of the enamel, dentin, and the pulp in the explored region (Fig. 1A). Micro-computed-tomography (micro-CT) of jaws in SAMP1/kl-deficient mice demonstrated that enamel was present from the cervical loop region. The shape and size of the distal incisors (dentin/enamel volume) was not significantly different between the SAMP1/kl+/+ and SAMP1/kl-deficient mice. Important differences were observed in the maturation of the root of the lower proximal incisors. The incisor root regions in SAMP1/kl -/- mice showed greater defects in mineralization and root canal calcification compared to SAMP1/kl+/+ mice. The sharpness of incisor tip in SAMP1/kl -/- mice was disappeared at 8 week, probably due to abrasion of enamel in labial side. In Histologic analysis, the tooth in SAMP1/kl-deficient mice showed irregular enamel space and distorted dentin structure (Fig. 1B), supporting a mineralization defect in tooth.

We showed a specific mandibular phenotype in the SAMP1/kl-/- mice compared to the SAMP1/kl+/+ by a micro-CT. Interestingly, the SAMP1/kl-/- mice exhibited an extremely

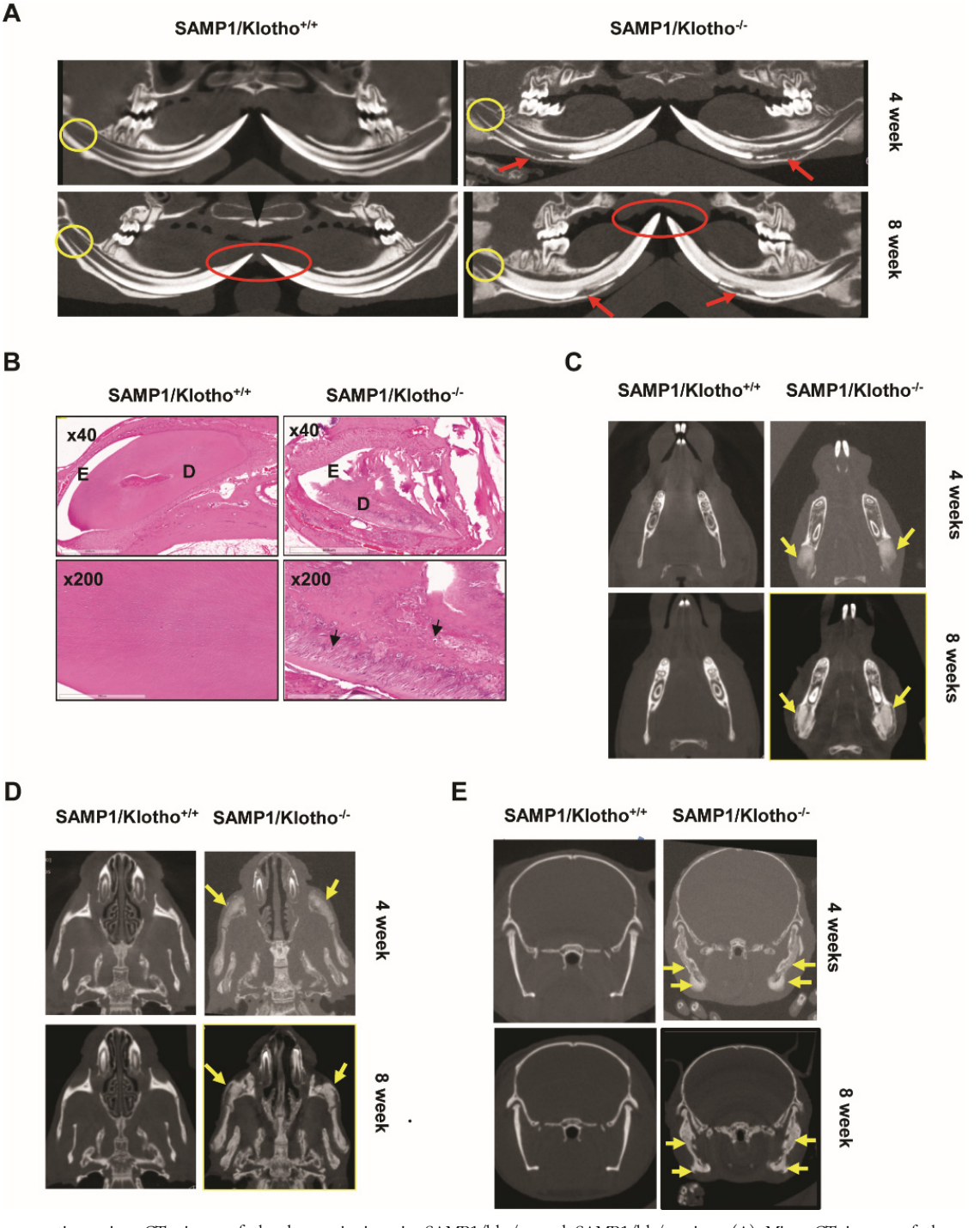

Fig. 1. Comparative micro-CT views of the lower incisor in SAMP1/kl+/+ and SAMP1/kl-/- mice. (A) Micro-CT image of the mandibular incisors from 4- or 8-week-old mice. Yellow and red circles denote cervical loop and tip of incisors. Red arrows indicate mineralization defect of enamel on labial side. (B) Histologic findings of tooth. The morphology of dentin (D) and enamel (E) in SAMP1/kl+/+ and SAMP1/kl-/- mice. Note entrapped odontoblast in dentinal tubules in Klotho-/- mice (arrows). Micro-CT image of the mandibular bone in SAMP1/kl+/+ and SAMP1/ kl-/- mice. (C) A region of the axial mandibular bone. The arrow indicates the mandibular ramus in the SAMP1/kl mice. (D) Image of the malar bone (arrow). (E) Image of the coronal mandibular bone. Arrows point to the mandible and mandibular ramus. All mice were 4 or 8 weeks old.

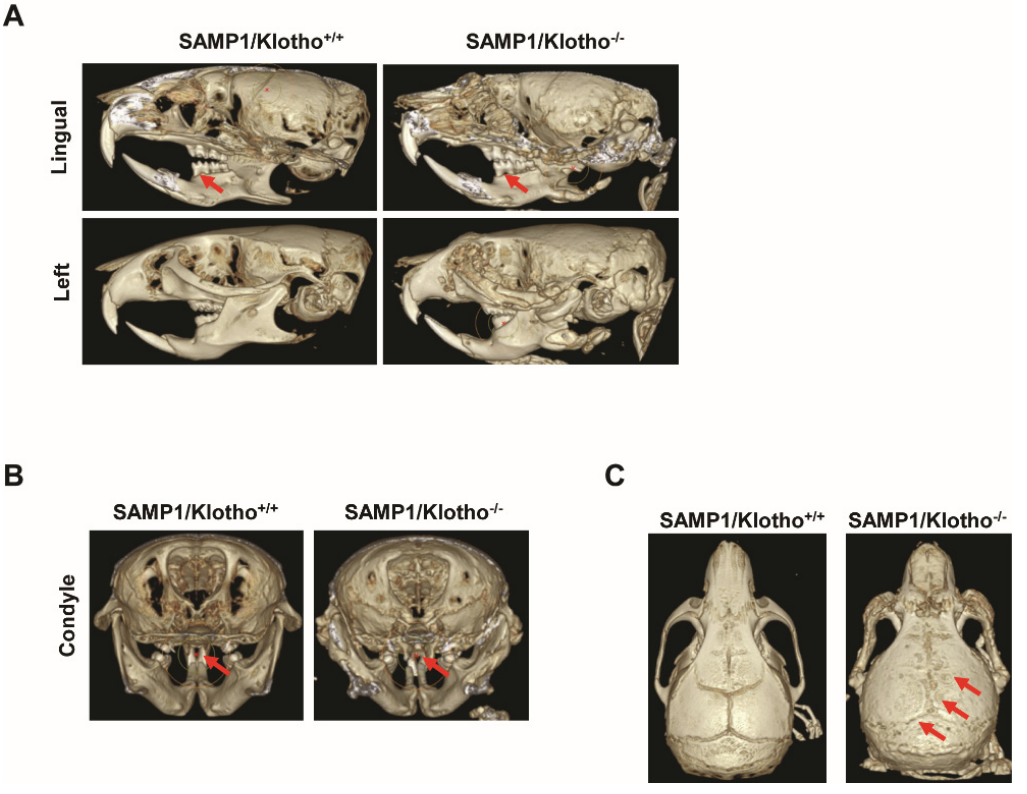

Fig. 2. 3D structural images were reconstructed for the head and neck of SAMP1/kl-/- and SAMP1/kl+/+ mice. Display of the different anatomical regions of mandibular bone: lower and upper incisors, nasal bone, frontal bone, parietal bone, intraparietal bone, left mandible and molars. (A) 3D surface renderings of micro-CT images of mandibular bone of 8 week-old aged mice: lingual bone images (up) and left head images (down). (B) 3D-image of the frontal view of mandibular bone. The arrow indicates the mandibular joint (condyle). (C) Three-dimensional surface renderings of micro-CT images showing the skull.

abnormal trabecular pattern (ground glass appearance) and loss of cortical bone in the inferior portion of both mandibular rami (Fig. 1C). In addition, the head and neck bones of the SAMP1/kl-/- mice were poorly mineralized and showed impaired bone development and an abnormal shape of the nasal conchae and ethmoidal labyrinth (Fig. 1D). In the SAMP1/kl-/- mice, the mandibular ramus width was thicker than that in SAMP1/kl+/+ mice (Fig. 1E).

2. Three-dimensional surface rendering of the head and neck bones of the SAMP1/kl-/- mice using micro-CT

We compared the phenotypic variation of the skeletal structures between SAMP1/kl+/+ and SAMP1/kl-/- mice. Three-dimensional surface rendering of micro-CT images revealed that the resorption of the alveolar bone on the lingual side, bone deposition on the ramus and thickness of the zygomatic bone were increased. (Fig. 2A). However, there were no significant differences in condylar formation between the SAMP1/kl+/+ and SAMP1/kl-/- mice (Fig. 2B). In addition, SAMP1/kl-/- mice were characterized by fused sutures (coronal, sagittal, lambdoid) of the skull compared to SAMP1/kl+/+ mice (Fig. 2C).

3. SAMP1/kl-deficient mice exhibited ectopic calcification in mandibular bone

The effect of SAMP1/kl deficiency on head and neck bone morphology was examined using hematoxylin and eosin staining in SAMP1/kl+/+ and SAMP1/kl-/- mice. The teeth in the

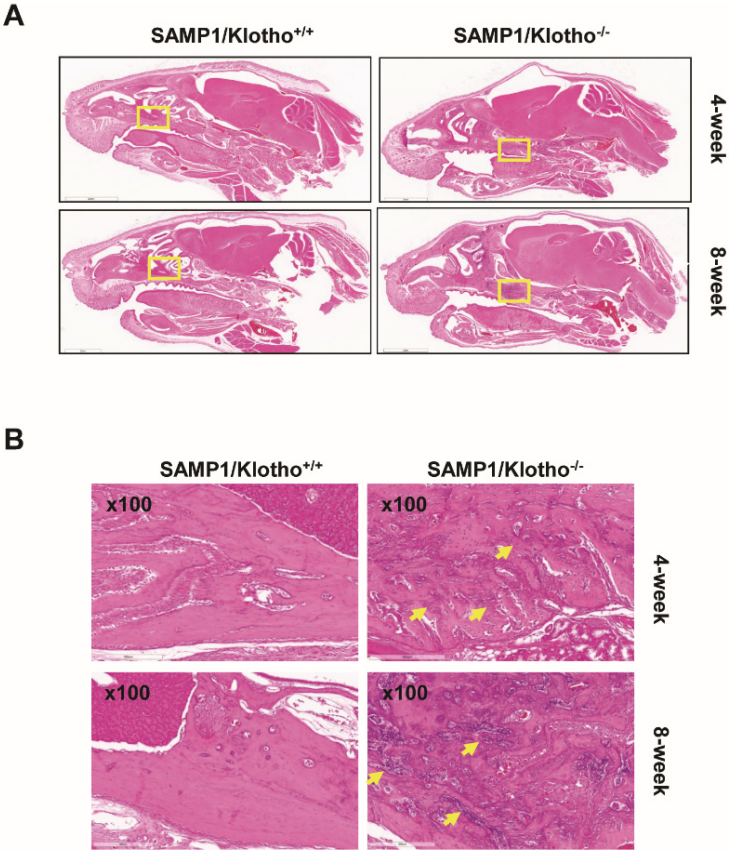

Fig. 3. Histological analysis of SAMP1/kl+/+ and SAMP1/kl-/- mice. (A) Representative sagittal sections of the head and neck of 4 or 8-week-old SAMP1/kl+/+ and SAMP1/kl-/- mice stained with hematoxylin and eosin (H&E). (B) Histological sections (H&E staining) of the maxillary bone (yellow boxed area in panel A) showing an irregular calcification (arrow) in the SAMP1/kl-/- mice.

SAMP1/kl-/- mice showed dysplastic dentin with irregular dentinal tubule formation, as well as resorption of the alveolar bone. In addition, discontinuous and thicker bones were observed around the nasal cavity (Fig. 3A). Immature bone trabeculae-like structures appeared at the ramus of the mandible in 4- and 8-week-old SAMP1/kl-/- mice. SAMP1/kl-/- mice also showed greater dysplastic bone with irregular calcification of the maxillary bone, facial bone, mandibular bone, and cranial bone compared to the SAMP1/kl+/+ mice (Fig. 3B).

4. The micro-CT analysis of the trabecular bones in distal femurs

To reveal the condition of the bone in SAMP1/kl-/- mice, we used micro-CT to analyze and compare the architecture of the vertebral column, tibia, and femoral trabecular and cortical bone. 3D reconstructions of the vertebral column of 2-month-old SAMP1/kl-/- mice revealed prominent kyphosis (curvature of the vertebral column) compared with SAMP1/kl+/+ mice (Fig. 4A). In the 2-month-old SAMP1/kl-/- mice, the tibia and femurs showed abnormal structures including enlarged and shortened femurs. The cortical bones of the femurs in the SAMP1/kl-/- mice showed irregularity and discontinuity and an internal granular appearance compared with those of the SAMP1/kl+/+ mice. In the SAMP1/kl-/- mice, the growth plate in the femoral head was closed, unlike that of SAMP1/kl+/+ mice (Fig. 4B). The 3D image showed that the number of trabecular bones in the SAMP1/kl-/- mice was substantially increased. Additionally, the SAMP1/

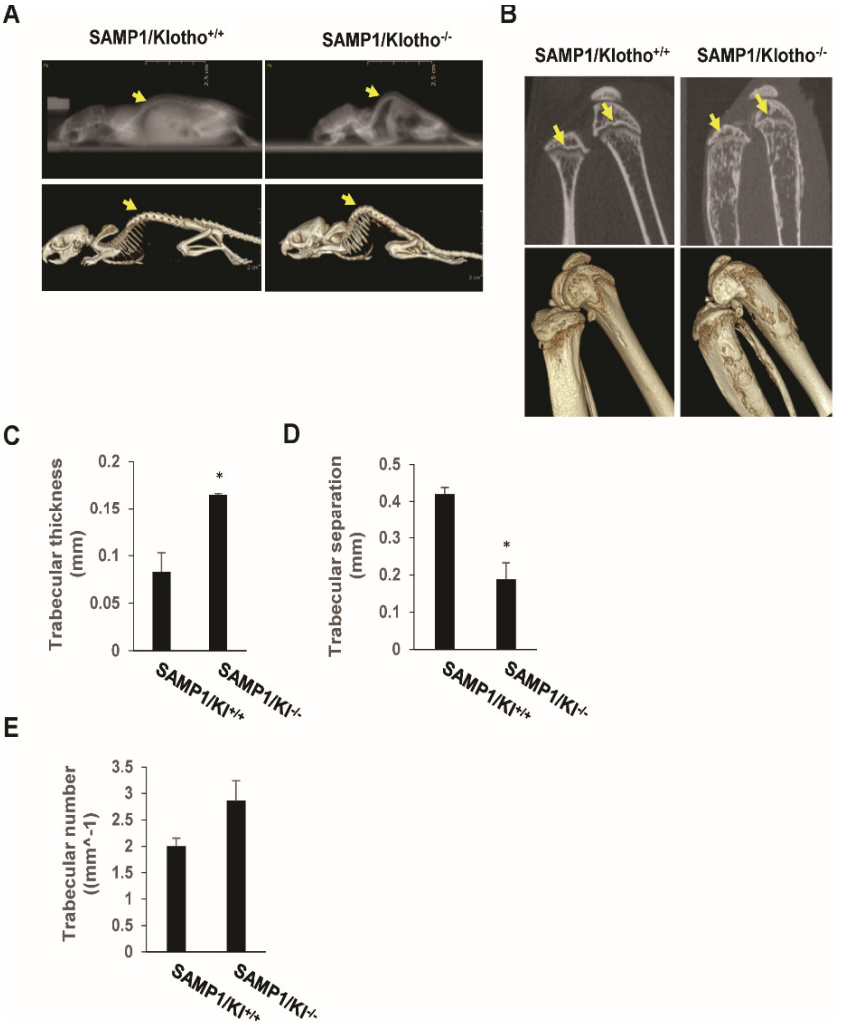

Fig. 4. Micro-CT analysis of the vertebral bones, tibia and femurs in SAMP1/kl+/+ and SAMP1/kl-/- mice. (A) Sagittal micro-CT (up) and 3D reconstruction (down) images showing vertebral kyphosis (arrow) in SAMP1/kl-/- mice at 8 weeks of age. (B) Coronal sections of the tibia and femurs of SAMP1/kl-/- mice. Arrows point to growth plate. (C-E) The micro-CT analytic scores of the trabecular bones of the femurs. The trabecular thickness (C), trabecular separation (D), and trabecular number (E) are shown. $^{*}p < 0.05$.

kl-/- mice revealed cortical bone thinning in the femur compared with the SAMP1/kl+/+ mice (Fig. 4B). Micro-CT analysis, which included bone volume (BV) / tissue volume (TV) and the number of trabecular bones (Tb.N), displayed results similar to those observed in the 3D structures. The separation (Tb.Sp) of the trabecular bone indicated that the spongy structures of the trabecular bone were decreased in the SAMP1/kl-/- mice and that the trabecular bone numbers were increased in the SAMP1/kl-/- mice (Fig. 4C-4E).

Ⅳ. DISCUSSION

In this study, we compared the characterization of head and neck bones between the SAMP1/kl+/+ and SAMP1/kl-deficient mice. Previously, Rangiani et al. reported that no obvious changes were evident in the overall incisor structure in Dmp1/Klotho deficient (Dmp1(-/-)kl/kl) mice[20,21]. However, using micro-CT analysis, we found that the microarchitecture of the 4 or 8-week-old SAMP1/kl -/- lower incisors displayed severe defects in tooth structures, including

loss of incisor roots, irregular dentinal tubule formation, as well as calcification within the pulp root canal. Furthermore, the mandibular ramus showed an extensive ground glass appearance in SAMP1/kl -/- compared with the age-matched SAMP1/kl +/+. In addition, the lower proximal incisors of the SAMP1/kl -/- mice showed a greater defect in tooth mineralization and a reduction of cementum thickness compared to those of the SAMP1/kl+/+ mice. However, the morphology of the distal incisors (dentin/enamel volume) was not significantly different between the SAMP1/kl+/+ and SAMP1/kl-/- mice. Unlike klotho +/+ mice, our study showed various unusual imaging findings in the SAMP1/kl-/- mice. Our micro-CT imaging showed a characteristic ground glass appearance, which had not been previously reported elsewhere in the literature on klotho -/- mice. We hypothesized that the ground glass appearance of the mandible observed in the micro-CT images may be correlated with acute bone inflammation, bone tumor, or calcification of the lesions. The ground glass appearance within the lesion could be an unusual micro-CT imaging finding for premature aging-like mandibular bone phenotypes. In the histological analysis, we found the development of the calcified bone structure and dysplastic bone formation to appear in a progressive fashion in the head & neck of SAMP1/kl -/- mice. Our results may provide an understanding of the pathologic alterations of aging-related bone development.

It has been suggested that Klotho deficient mice showed the characteristic bone phenotypes such as decreased bone mineral density, reduced trabecular and cortical thickness, lower trabecular and cortical bone volume and a severely reduced trabecular bone fraction[22,23].

In this study, we explored the morphological differences in the vertebral column, tibia, and femurs caused by a SAMP1/klotho deficiency using 3D reconstructions of the micro-CT. We observed (i) prominent kyphosis (curvature of the vertebral column), (ii) irregularity and discontinuity in the cortical bones of the femurs, (iii) a closed growth plate in the femoral head, and (iv) reduced separation of the trabecular bone, collectively providing results for insufficient trabecular and cortical bone structure of the femur. However, the bone mineral density (BMD) of the trabecular bones did not change significantly in the SAMP1/kl-/- mice compared with the SAMP1/kl+/+ mice. Additionally, we observed an increased bone volume and trabecular thickness in the SAMP1/kl-/- mice. We supposed that decreased the sponge structure of the trabecular bone could increase the trabecular number and thickness as a compensatory measure because it weakens the bones. Interestingly, a micro-CT analysis that included bone mineral density, bone volume, and trabecular thickness displayed differences in klotho-/- mice and in SAMP1/kl-/- mice even though the body phenotypes were similar. Although we could not exactly provide the explanation for these observations in the SAMP1/kl-/- mice, they may reflect the different bone formation/turnover or abnormal increased immature bone compared with that of klotho-/- mice.

In conclusion, SAMP1/kl-/- mice displayed a rapid induction of osteodystrophy and/or other bone diseases including unnecessary trabecular and cortical bone mass at a young age (4 and 8 weeks old). SAMP1/kl-/- mice also showed greater dysplastic bone with irregular calcification of the maxillary bone, facial bone, mandibular bone, and cranial bone compared to the SAMP1/kl+/+ mice. We conclude that SAMP1/kl-/- mice may serve as a useful model to mimic the development of osteodystrophy due to bone growth rather than bone resorption.

ACKNOWLEDGEMENTS

This work was supported by the National Research Foundation of Korea (NRF) grant funded by the Korean government (MSIT) (no. 2018052384).

REFERENCES

1. López-Otín C, Blasco MA, Partridge L, Serrano M, Kroemer G: The hallmarks of aging. Cell 2013;153: 1194-217.
2. Demontiero O, Vidal C, Duque G: Aging and bone loss: New insights for the clinician. Ther Adv Musculoskelet Dis 2012; 4:61-76.
3. Takeda T, Matsushita T, Kurozumi M, Takemura K, Higuchi K, Hosokawa M: Pathobiology of the senescence-accelerated mouse (SAM). Exp Gerontol 1997;32:117-127.
4. Chang S, Multani AS, Cabrera NG, Cabrera NG, Naylor ML, Laud P, Lombard D, Pathak S, Guarente L, DePinho RA: Essential role of limiting telomeres in the pathogenesis of Werner syndrome. Nat Genet 2004;36:877-882.
5. Kuro-o M, Matsumura Y, Aizawa H, Kawaguchi H, Suga T, Utsugi T, Ohyama Y, Kurabayashi M, Kaname T, Kume E, Iwasaki H, Iida A, Shiraki-Iida T, Nishikawa S, Nagai R, Nabeshima YI: Mutation of the mouse klotho gene leads to a syndrome resembling ageing. Nature 1997;390:45-51.
6. Kurosu H, Ogawa Y, Miyoshi M, Yamamoto M, Nandi A, Rosenblatt KP, Baum MG, Schiavi S, Hu MC, Moe OW, Kuro-o M: Regulation of fibroblast growth factor-23 signaling by klotho. J Biol Chem 2006;281:6120-6123.
7. Kuro-o M: Klotho as a regulator of fibroblast growth factor signaling and phosphate/calcium metabolism. Curr Opin Nephrol Hypertens 2006;15:437-441.
8. Nakatani T, Sarraj B, Ohnishi M, Densmore MJ, Taguchi T, Goetz R, Mohammadi M, Lanske B, Razzaque MS: In vivo genetic evidence for klotho-dependent, fibroblast growth factor 23 (Fgf23)-mediated regulation of systemic phosphate homeostasis. FASEB J 2009;23:433-441.
9. Urakawa I, Yamazaki Y, Shimada T, Iijima K, Hasegawa H, Okawa K, Fujita T, Fukumoto S, Yamashita T: Klotho converts canonical FGF receptor into a specific receptor for FGF23. Nature 2006;444:770-774.
10. Doi S, Zou Y, Togao O, Pastor JV, John GB, Wang L, Shiizaki K, Gotschall R, Schiavi S, Yorioka N, Takahashi M, Boothman DA, Kuro-o M: Klotho inhibits transforming growth factor-beta1 (TGF-beta1) signaling and suppresses renal fibrosis and cancer metastasis in mice. J Biol Chem 2011;286:8655-8665.
11. Sopjani M, Rinnerthaler M, Kruja J, Dermaku-Sopjani M: Intracellular signaling of the aging suppressor protein Klotho. Curr Mol Med 2015;15:27-37.
12. Komaba H., Kaludjerovic J, Hu DZ, Nagano K, Amano K, Ide N, Sato T, Densmore MJ, Hanai JI, Olauson H, Bellido T, Larsson TE, Baron R, Lanske B: Klotho expression in osteocytes regulates bone metabolism and controls bone formation. Kidney Int 2017;92:599-611.
13. Kawaguchi H, Manabe N, Miyaura C, Chikuda H, Nakamura K, Kuro-o M: Independent impairment of osteoblast and osteoclast differentiation in klotho mouse exhibiting low- turnover osteopenia. J Clin Invest 1999;104:229-237.
14. Kuro-O M: The FGF23 and Klotho system beyond mineral metabolism. Clin Exp Nephrol 2017;21:64-69.
15. Yamashita T, Nabeshima Y, Noda M: High-resolution micro-computed tomography analyses of the abnormal trabecular bone structures in klotho gene mutant mice. J Endocrinol 2000;164:239-245.
16. Liu H, Fergusson MM, Castilho RM, Liu J, Cao L, Chen J, Malide D, Rovira II, Schimel D, Kuo CJ, Gutkind JS, Hwang PM, Finkel T: Augmented Wnt signaling in a mammalian model of accelerated aging. Science 2007;317:803-806.
17. Yuan Q, Sato T, Densmore M, Saito H, Schüler C, Erben RG, Lanske B: Deletion of PTH rescues skeletal abnormalities and high osteopontin levels in Klotho-/- mice. PLOS Genetics 2012, 8:e1002726.
18. Kim SA, Lam TG, Yook, JI, Ahn SG: Antioxidant modifications induced by the new metformin derivative HL156A regulate metabolic reprogramming in SAMP1/kl (-/-) mice. Aging (Albany NY) 2018;10:2338-2355.
19. Takeda T: Senescence-accelerated mouse (SAM): A biogerontological resource in aging research. Neurobiol Aging 1999;20:105-110.
20. Rangiani A, Cao ZG, Liu Y, Voisey Rodgers A, Jiang Y, Qin CL, Feng JQ: Dentin matrix protein 1 and phosphate homeostasis are critical for postnatal pulp, dentin and enamel formation. Int J Oral Sci 2012a;4:189-95.
21. Rangiani, A, Cao Z, Sun Y, Lu Y, Gao T, Yuan B, Rodgers

A, Qin C, Kuro-O M, Feng JQ: Protective roles of DMP1 in high phosphate homeostasis. PLoS One 2012b;7:e42329.
22. Jernvall J, Thesleff I: Tooth shape formation and tooth renewal: evolving with the same signals. Development 2010; 139:3487-3497.
23. Seidel K, Ahn CP, Lyons D, Nee A, Ting K, Brownell I, Cao T, Carano RA, Curran T, Schober M, Fuchs E, Joyner A, Martin GR, de Sauvage FJ, Klein OD: Hedgehog signaling regulates the generation of ameloblast progenitors in the continuously growing mouse incisor. Development 2010;137: 3753-3761.